

The oxidation state at tunnel junction interfaces

X. Batlle^{a)}, B.J. Hattink, A. Labarta

Dept. Física Fonamental, Univ. Barcelona, Av. Diagonal 647, 08028-Barcelona, Catalonia, Spain

B.J. Jönsson-Åkerman, R. Escudero^{b)}, I.K. Schuller

University of California — San Diego, Physics Department-0319, La Jolla, CA 92093-0319, USA

(November 18, 2018)

We demonstrate that at the usual 10^{-7} torr range of base pressures in the sputtering chamber, X-ray photoelectron spectroscopy shows the existence of a thin AlO_x layer at the Nb/Al interface in both Nb/Al- AlO_x /Pb tunnel junctions and Nb/Al bilayers. This is due to the time elapsed between the deposition of the Nb and Al bottom layers, even at times as short as 100 s. We also give some direct evidence of the oxidation of the top Pb electrode on the Nb electrode surface. Such oxidation probably occurs at the pinholes of the intermediate Al- AlO_x layer of the junctions, as a consequence of the oxidation state at the Nb/Al interface. We therefore suggest that both the base pressure and the time lapse between layer depositions should be carefully controlled in magnetic tunnel junctions.

75.70.-i; 73.40.Gk; 74.50.+r; 73.50.Jt; 85.30.Mn; 85.70.Kh

Ferromagnet/insulator/ferromagnet (FM/I/FM) magnetic tunnel junctions (MTJs) exhibiting large magnetoresistance (MR)¹ have lately attracted much interest due to their potential applications^{2,3}. The performance of the junctions is strongly dependent on the oxidation of the FM electrodes at the FM/I interfaces, as well as on the oxidation state of the barrier, which has to be homogenous and complete. The use of thinner and thinner barriers has reopened the question of how to rule out the presence of pinholes. Rowell and others developed a set of criteria to ascertain that tunneling is the dominant mechanism in junctions with at least one superconducting (S) electrode⁴. Three of these criteria still apply in FM/I/FM structures: (i) an exponential insulator thickness dependence of the conductance, G ; (ii) a parabolic voltage dependence of G that can be fitted to the theoretical models^{5,6}; and (iii) a weak insulating-like dependence $G(T)$.

For the first criterion, it has been shown⁷ that pinholes may mimic the exponential thickness dependence of the tunneling resistance. For the second one, some of us demonstrated⁸ that S/I/FM junctions that displayed parabolic $G(V)$ curves in the normal state, showed, at low temperatures and depending on the oxidation procedure, either tunneling or pinhole conduction (Andreev reflection⁹). The recent observation of very large MR in Co-Co and Ni-Ni wire nanocontacts¹⁰ also suggests the pinhole contribution to TMR in MTJs. Given the ratio of the conduction between metallic contacts and junctions¹¹, pinhole regions of one part in 10^6 must be

ruled out to ensure no pinhole conduction in parallel with tunneling. For the third criterion, some results suggest that pinholes yield a metallic-like temperature dependence of the junction resistance^{8,12}. Therefore, out of the three Rowell criteria, only one, the insulating-like $G(T)$, seems to be reliable.

X-ray photoelectron spectroscopy (XPS)¹³ is an excellent technique for the analysis of MTJs¹⁴ since it is sensitive to the chemical species as well as to their bonding state. In this letter, we show that at the usual 10^{-7} torr range of base pressures in the sputtering chamber, XPS indicates that there exists a thin oxygen layer mostly adsorbed on the surface of the bottom electrode that yields the oxidation of the first impinging atoms of the intermediate layer. We also demonstrate that this is due to the time elapsed between the deposition of the layers. Therefore, the oxidation state at the interfaces strongly affects the tunneling process by modifying the pinhole conductivity and the interface chemistry and roughness.

The junctions were prepared as follows⁸: a dc sputtered superconducting Nb(80 nm)/Al(10 nm) bilayer bottom electrode was oxidized in air 10 minutes and a Pb top electrode (200 nm) was deposited in a separate thermal evaporation unit, leading to the Nb/Al- AlO_x /Pb junction (Pb sample). The resulting oxide thickness was typically 1-2 nm and the remaining 8 nm of metallic Al were superconducting for proximity to the Nb¹⁵. For a second sample, the bottom electrode was oxidized for 18 hours in air (barrier thickness of 2-3 nm) and a Ni (20 nm) layer was dc sputtered on top, leading to the Nb/Al- AlO_x /Ni junction (Ni sample). The junction area for both samples was $1 \times 0.3 \text{ mm}^2$. These two samples are representative of the variety of samples studied⁸. Standard ac (1 kHz) differential conductance $G = dI/dV$ measurements as a function of dc bias were carried out from 4.2 to 300 K using a balanced bridge. XPS spectra (Al K_{α} ; base pressure 10^{-9} torr) were recorded for exactly the same samples as in $G(V)$. The distribution of elements across the junction was studied by performing a low-energy sputtering process (4 keV, incident at 45° ; typical etching rate 6-10 nm/minute) for a short time (6-18 s) and recording the spectrum after each step. This sputtering process, which may lead to a certain intermixing, together with the fact that the XPS signal averages the out-coming electrons from a region of about 5-10 nm in depth, precludes the observation of sharp interfaces.

For the Pb junction, $G(V)$ at 155 K suggests tunnel

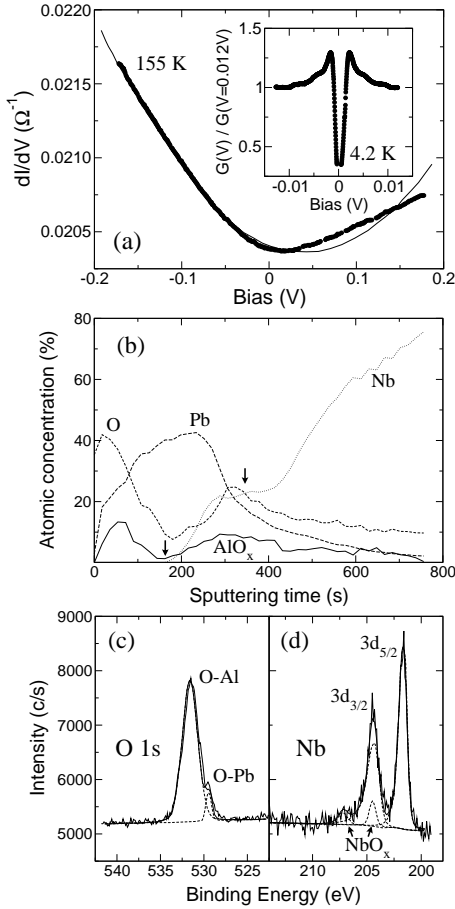


FIG. 1. Nb/Al- AlO_x /Pb junction: (a) $G(V)$ curve at 155 K, together with a fit to the BDR model. Inset: $G(V)$ curve at 4.2 K, showing the superconducting gap (tunnel conduction). (b) Atomic concentration obtained from the XPS intensities for Pb, O, AlO_x and Nb, as a function of the sputtering time. (c) Example of the XPS spectra for the O 1s core level at the Nb/Al interface (sputtering time: 324 s), showing the O-Al and O-Pb (3%) contributions. (d) Nd 3d core level (sputtering time: 216 s), showing the NbO contribution.

conduction (Fig. 1(a)), which is confirmed by the signature of the superconducting gap at 4.2 K (inset of Fig. 1(a)). The fit of $G(V)$ to the Brinkman-Dynes-Rowell (BDR) model⁵ yields a barrier thickness of 1.1 nm and heights of 3.6 eV and 2.4 eV on the Pb and Nb/Al sides, respectively, while the fit to the Simmons' model⁶ yields 1.2 nm and 2.9 eV. For the Ni sample, G is high and flat, indicating big metal-to-metal shorts. This suggests that Pb mostly adds to the AlO_x barrier without damaging it and that the latter is free of metal-to-metal pinholes. However, Ni damages the barrier, in agreement with previous studies of the influence of the top electrode on the junction properties: both the junction resistance¹⁶ and the barrier height¹⁷ increase with the ionic radius (from Ni to Pb) since the larger the latter is, the less the element can penetrate in the barrier, resulting in less effective micro-shorts.

Fig. 1(b) shows the atomic concentration of Nb, Pb, AlO_x and O obtained from the XPS intensities¹³ for the Pb sample, as a function of the sputtering time (sputtering steps of 18 s). The AlO_x concentration was obtained by fitting the intensity of the Al 2p core level to both a metallic and oxide contribution¹³. As soon as Nb is detected, the O signal increases, first reaching a maximum and later decreasing as the sputtering process approaches the Nb layer. The AlO_x concentration perfectly follows that of O (Fig. 1(b)), the first maximum corresponding to the insulating barrier, the second one (ca. 300 s) suggesting that there is a thin oxygen layer on top of Nb that oxidizes the first Al atoms arriving at the bottom electrode. At short sputtering times, the oxidation of both the free surface of the sample (O-Pb 1s at 528.3-529.4 eV) and the barrier (O-Al 1s at 531-531.5 eV) are observed. Besides, the O-Al 1s peaks at the Nb/Al interface are clearly asymmetric at low energies, and a small peak at about 529.3 eV is observed (Fig. 1(c)), suggesting an O-Pb contribution of about 3%. This indicates that some PbO_x is present on the Nb surface, which is probably due both to the existence of the oxygen layer at the Nb/Al interface and to the consequent Pb oxidation at the pinholes of the Al- AlO_x layer. This is in agreement with some electron microscopy studies showing a pinhole surface area up to about 2% in AlO_x barriers¹⁸, even if in the present Pb junction, the former Al layer was about 10 nm in thickness. From the Nb 3d core level (Fig. 1(d)), some NbO (Nb-O $3d_{5/2}$ at 204.6 eV) on the surface of the Nb layer is inferred, although the calculated O-Nb contribution is at least one order of magnitude smaller than the experimental O-Al one, so that the former (530.0-530.4 eV) is not detected since it overlaps to the latter. The Pb 4f core level (not shown) at the Nb/Al interface also yields a small amount of PbO and/or Pb_3O_4 , while the O-Pb/Pb-O ratio is about 1.5. The Ni sample also follows this framework: both the O-Al 1s and Al-O 2p signals increase on the surface of Nb.

Given the base pressures in the sputtering chamber (2.6×10^{-7} and 1.3×10^{-7} torr for the Pb and Ni samples, respectively), the thin oxygen layer at the Nb/Al interface is related to the time that the Nb film is kept in the chamber before the Al deposition proceeds (45 minutes and 5 hours for the Pb and Ni junctions, respectively). Three Nb(100 nm)/Al(20 nm) bilayers were prepared to support this suggestion: sample Nb/Al-1, for which the Nb layer was 100 s in chamber (base pressure of 1.4×10^{-7} torr); sample Nb/Al-2, for which the Nb layer was 18.5 hours in the chamber (1.2×10^{-7} torr); and sample Nb/Al-3, for which the Nb layer was 27 hours in air (former base pressure of 1.4×10^{-7} torr). The role of the standard Gibbs energy of formation of the metal oxides ($\Delta_f G_0$ at 298.15 K)¹⁹ was studied by preparing two Nb(100 nm)/Pb(200 nm) bilayers with increasing transfer time in air from the sputtering chamber to the Pb evaporation unit; sample Nb/Pb-1 was 7 minutes in air, while sample Nb/Pb-2, was 24 hours.

The atomic concentration for Nb, metallic Al, O and

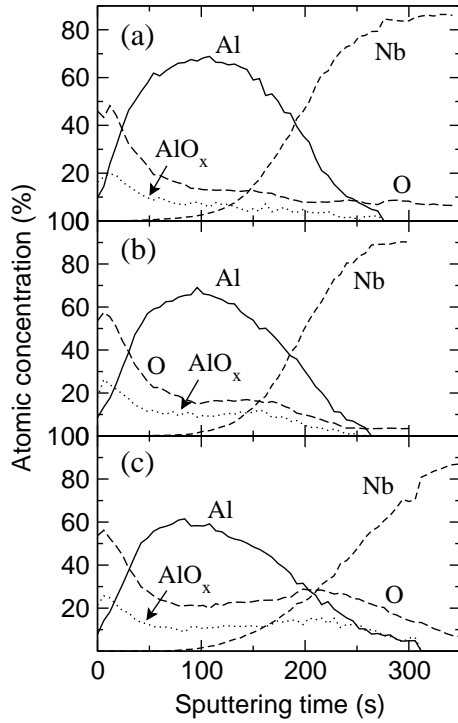


FIG. 2. (a) Atomic concentration obtained from the XPS intensities for Al, O, AlO_x and Nb, as a function of the sputtering time, for sample Nb/Al-1 (Nb layer kept 100 s in the sputtering chamber; base pressure of 1.4×10^{-7} torr). (b) Same data for sample Nb/Al-2 (18.5 hours, 1.2×10^{-7} torr). (c) Same data for sample Nb/Al-3 (27 hours in air).

AlO_x for the Nb/Al bilayers is shown in Fig. 2 as a function of the sputtering time (sputtering step of 6 s). The AlO_x concentration at the Nb/Al interface clearly increases with increasing time between the Nb and Al depositions. Even for sample Nb/Al-1 (Fig. 2(a)), there is change in the slope of both the concentrations of AlO_x and O as the Nb layer is detected. The O 1s core level yields mostly O-Al bonds and, although there might be some NbO on the surface of the Nb, the calculated O-Nb contribution is at least about one order of magnitude smaller than the O-Al one for all samples, in agreement with $\Delta_f G_0(\text{Al}_2\text{O}_3) = -1582.3$ kJ/mol and $\Delta_f G_0(\text{NbO}) = -378.6$ kJ/mol¹⁹. A similar picture is drawn for the Nb/Pb samples (not shown), the main differences being that, while at the free surface of the samples the oxidation state corresponds to O-Pb, in agreement with the Pb-O contribution to the Pb 4f core level, the O 1s increase at the Nb/Pb interface takes place at 530.0-530.4 eV, suggesting that this is the core level energy for the O-Nb 1s bonds. Both the Nb-O peak position and the O-Nb/Nb-O ratio at the Nb/Pb interfaces, suggest NbO_2 . Besides, the calculated O-Pb contribution is about two orders of magnitude smaller than the O-Nb one, in agreement with $\Delta_f G_0(\text{NbO}_2) = -740.5$ kJ/mol and $\Delta_f G_0(\text{PbO}) = -187.9$ kJ/mol¹⁹.

In conclusion, we have shown that when preparing tun-

nel junctions at the usual 10^{-7} torr base pressures, the oxidation state at the interfaces depends on the time elapsed between the deposition of the layers, even at times as short as 100 s, which is most relevant for the performance of the junctions. We therefore suggest that both parameters should be carefully controlled. We have also given some direct evidence of the oxidation of the top electrode on the surface of the bottom one, probably at the pinholes of the intermediate layer—even if the latter is about 10 nm in thickness—and due to the oxidation state at the interfaces. As some junctions studied show tunnel conduction, the oxidation state at the interfaces may be relevant to the dominant conduction mechanism. Consequently, the oxidation of the top FM layer at the pinholes of the insulating barrier in MTJs may well be influenced by the synthesis conditions so that the role of the latter in the quality of the junctions should be taken into account, the relative metal oxide formation energy of the selected elements being crucial.

Financial support of the Spanish CICYT (MAT2000-0858) and the Generalitat de Catalunya (ACI2000-04 and 2000SGR-025) are gratefully recognized. IKS acknowledges US DARPA and ONR.

-
- ^{a)} Corresponding author: xavier@ffn.ub.es
^{b)} Permanent address: IIM-UNAM, Mexico City, D.F. Apartado Postal 70-360, Mexico.
- ¹ J.S. Moodera, L.R. Kinder, T.M. Wong, and R. Meservey, *Phys. Rev. Lett.* **74**, 3273 (1995).
 - ² J.M. Daughton, *J. Appl. Phys.* **81**, 3758 (1997).
 - ³ W.J. Gallagher, S.S.P. Parkin, Y. Lu, X.P. Bian, A. Marley, K.P. Roche, R.A. Altman, S.A. Rishton, C. Jahnes, and T.M. Shaw, *J. Appl. Phys.* **81**, 3741 (1997).
 - ⁴ *Tunneling Phenomena in Solids*, edited by E. Burnstein and S. Lundqvist (Plenum, New York, 1969)
 - ⁵ W.F. Brinkman, R.C. Dynes, and J.M. Rowell, *J. Appl. Phys.* **41**, 1915 (1970).
 - ⁶ J.G. Simmons, *J. Appl. Phys.* **34**, 1793 (1963)
 - ⁷ D.A. Rabson, B.J. Jönsson-Åkerman, A.H. Romero, R. Escudero, C. Leighon, S. Kim and I.K. Schuller, *J. Appl. Phys.* **89** (in press, 1 March 2001).
 - ⁸ B.J. Jönsson-Åkerman, R. Escudero, C. Leighon, S. Kim and I.K. Schuller, *Appl. Phys. Lett.* **77**, 1870 (2000).
 - ⁹ G.E. Blonder, M. Tinkham, and T.M. Klapwijk, *Phys. Rev. B* **25**, 4515 (1982).
 - ¹⁰ G. Tatara, Y.W. Zhao, M. Muñoz, and N. García, *Phys. Rev. Lett.* **83**, 2030 (1999) and references therein.
 - ¹¹ W.P. Pratt, Jr., S.-F. Lee, J.M. Slaughter, R. Loloee, P.A. Schoeder and J. Bass, *Phys. Rev. Lett.* **66**, 3060 (1991).
 - ¹² U. Ruediger, R. Calarco, U. May, K. Samm, H. Kittur and G. Guentherodt, *J. Appl. Phys.* (in press, May 2001).
 - ¹³ *Practical Surface Analysis*, edited by D. Briggs and M.P. Seah (John Wiley, 1983).

- ¹⁴ S.R. Qiu, H.F. Lai and J.A. Yarmoff, Phys. Rev. Lett. **85**, 1492 (2000).
- ¹⁵ A. Zehnder, Ph. Lerch, S.P. Zhao, Th. Nussbaumer, E.C. Kirk, and H.R. Ott, Phys. Rev. B **59**, 8875 (1999).
- ¹⁶ R.M. Handy, Phys. Rev. **126**, 1968 (1962).
- ¹⁷ Y.B. Ning, M.C. Gallagher, and J.G. Adler, Phys. Rev. B **37**, 6139 (1988).
- ¹⁸ D. Ozkaya, R.E. Dunin-Borkowski, A.K. Petford-Long, P.K. Wong, and M.G. Blamire, J. Appl. Phys. **87**, 5200 (2000)
- ¹⁹ *CRC Handbook of Chemistry and Physics*, Boca Raton FL. Ed., CRC Press 1997 (78th ed.).